

$b_1(1235)$ Photoproduction at GlueX

**JLUO Annual Meeting
June 23, 2026**

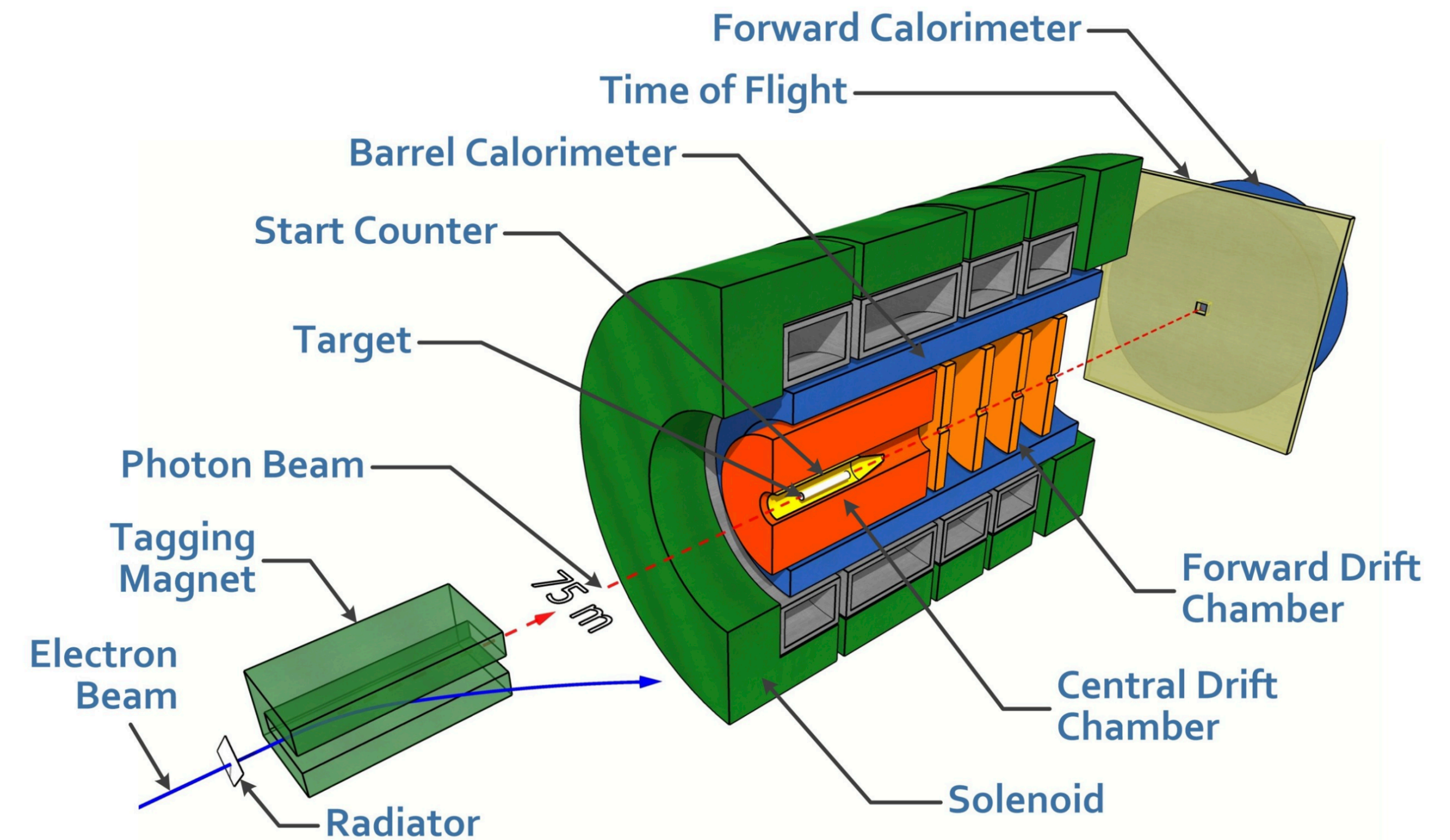


Amy M. Schertz (Indiana University)

GlueX

Polarized Photoproduction Experiment in Hall D

- Goal: measure and understand the light quark meson spectrum, search for exotic mesons
- Linear polarization ($\sim 35\%$) allows insight into production mechanisms
- Near-hermetic acceptance allows reconstruction and analysis of exclusive final states
- Large dataset collected by three experimental phases allows study of broad range of physics
 - GlueX-I: $\mathcal{L} = 125 \text{ pb}^{-1}$ (these results)
 - GlueX-II (ongoing): $\mathcal{L} \sim 3x$ GlueX-I (so far)
 - GlueX-III (2027+): $\mathcal{L} \sim 3x$ GlueX-I,II (projection)



GlueX: NIM A 987, 164807 (2021)

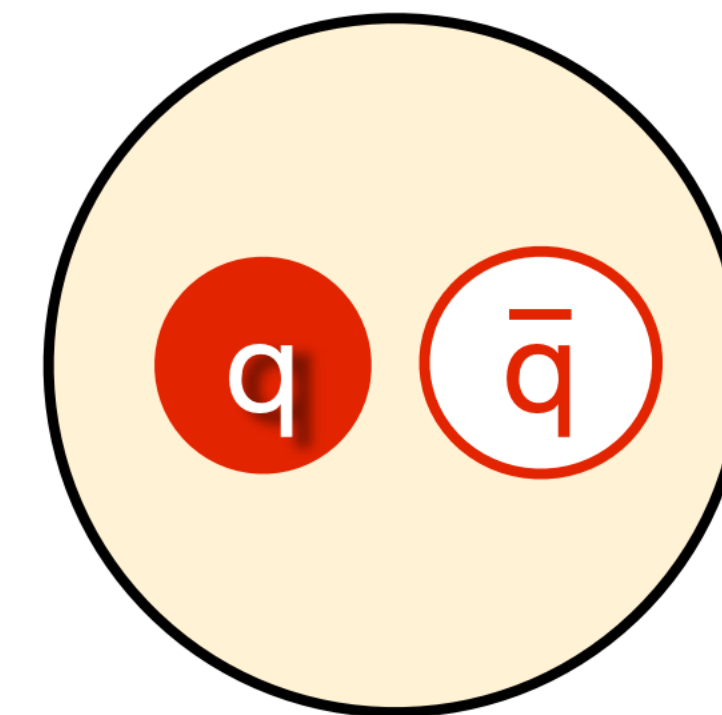
Exotic Mesons

- QCD allows for hybrid mesons, which have gluonic degrees of freedom contributing to the wavefunction
 - Allows for exotic quantum numbers, forbidden to $q\bar{q}$ pair
 - $J^{PC} = 0^{--}, 0^{+-}, 1^{-+}, 2^{+-}, \dots$
- Exotic quantum numbers are a “smoking gun” for non- $q\bar{q}$ systems
- NB: Not all hybrid mesons have exotic quantum numbers!

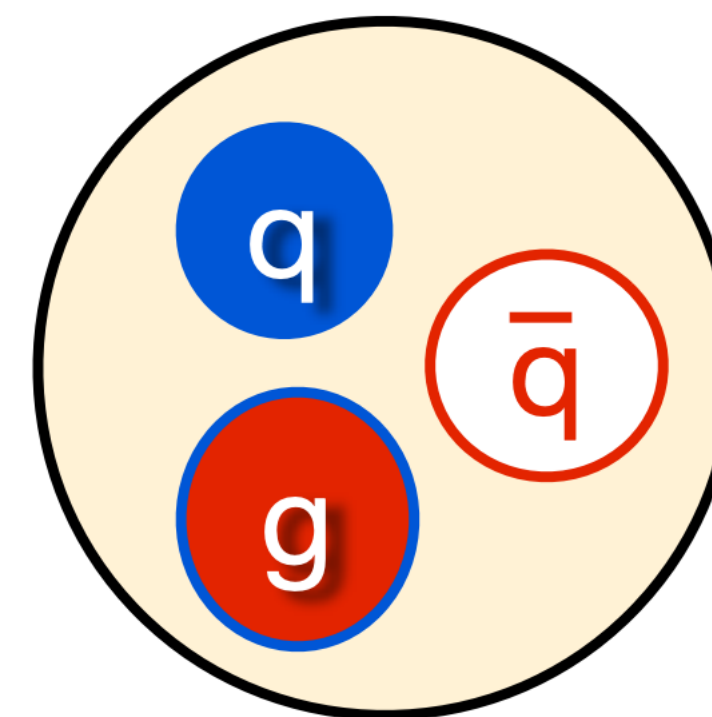
$$J = \left| \vec{L} + \vec{S} \right|$$

$$P = (-1)^{L+1}$$

$$C = (-1)^{L+S}$$



Meson

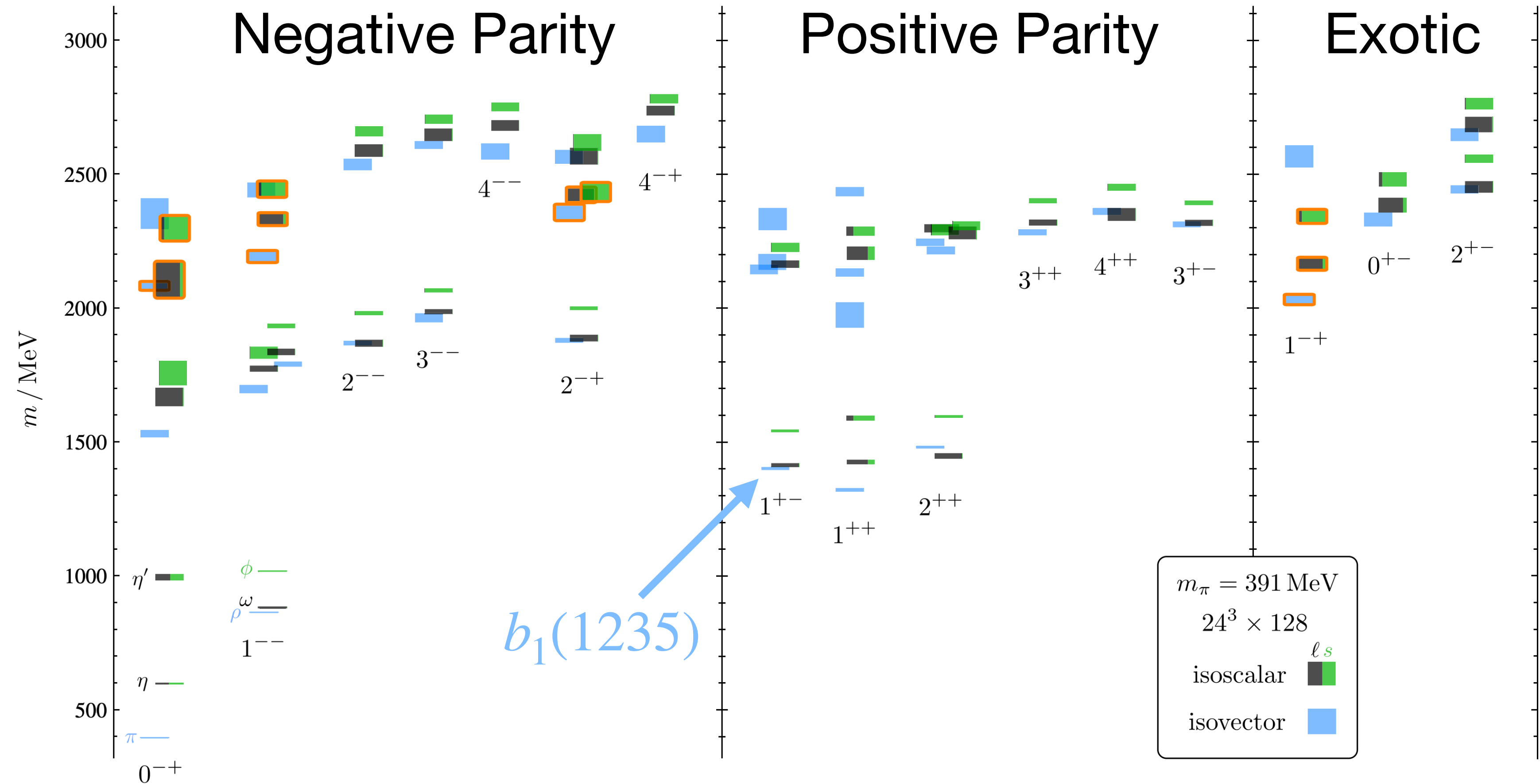


Hybrid Meson

Lattice QCD

Mass Spectrum of Light Quark Mesons

- Lattice calculation from first principles QCD indicates presence of hybrid mesons
- Orange outlines identify supermultiplet of lowest-lying hybrids

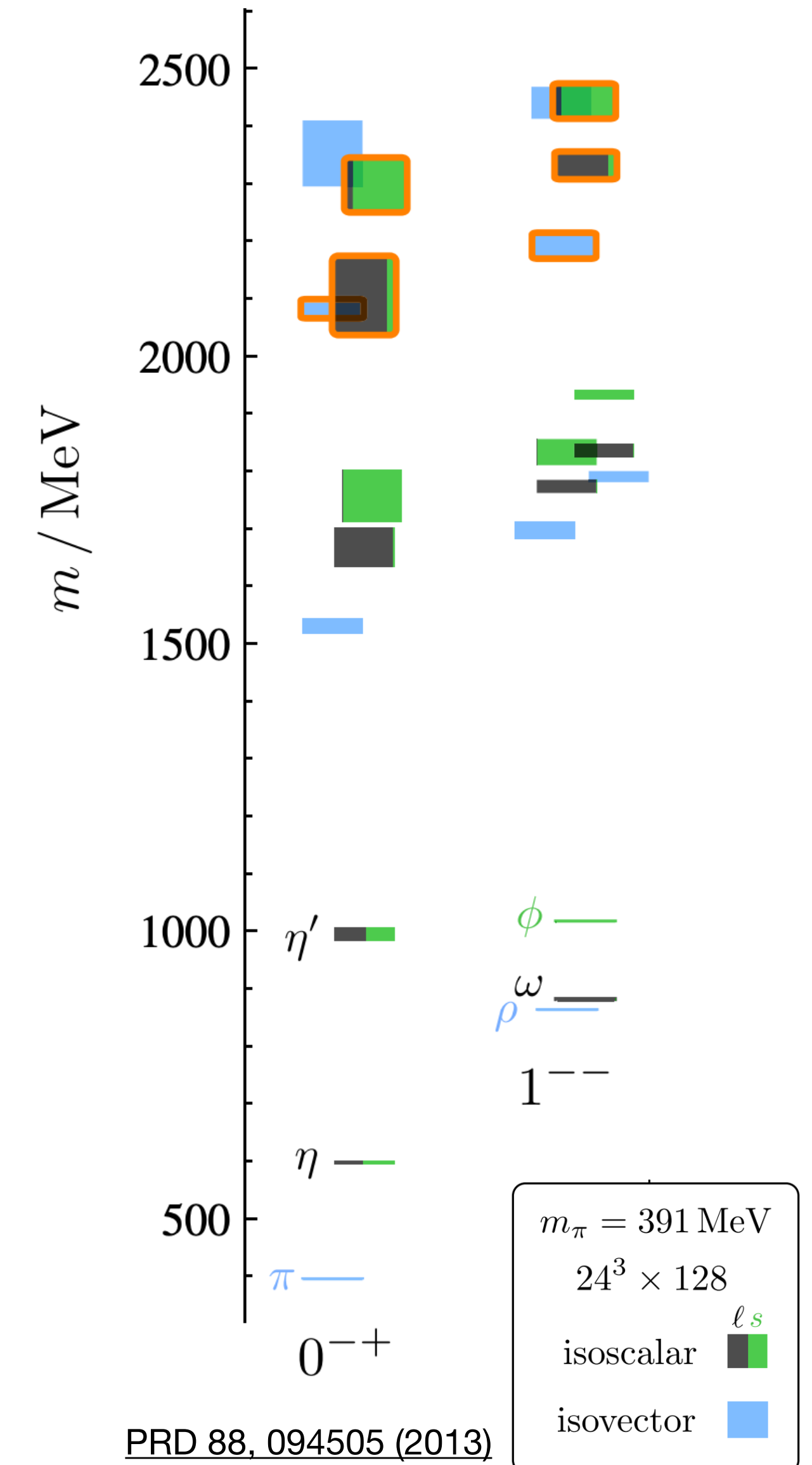


PRD 88, 094505 (2013)

Why Analyze the b_1 ?

We're interested in hybrids, right?

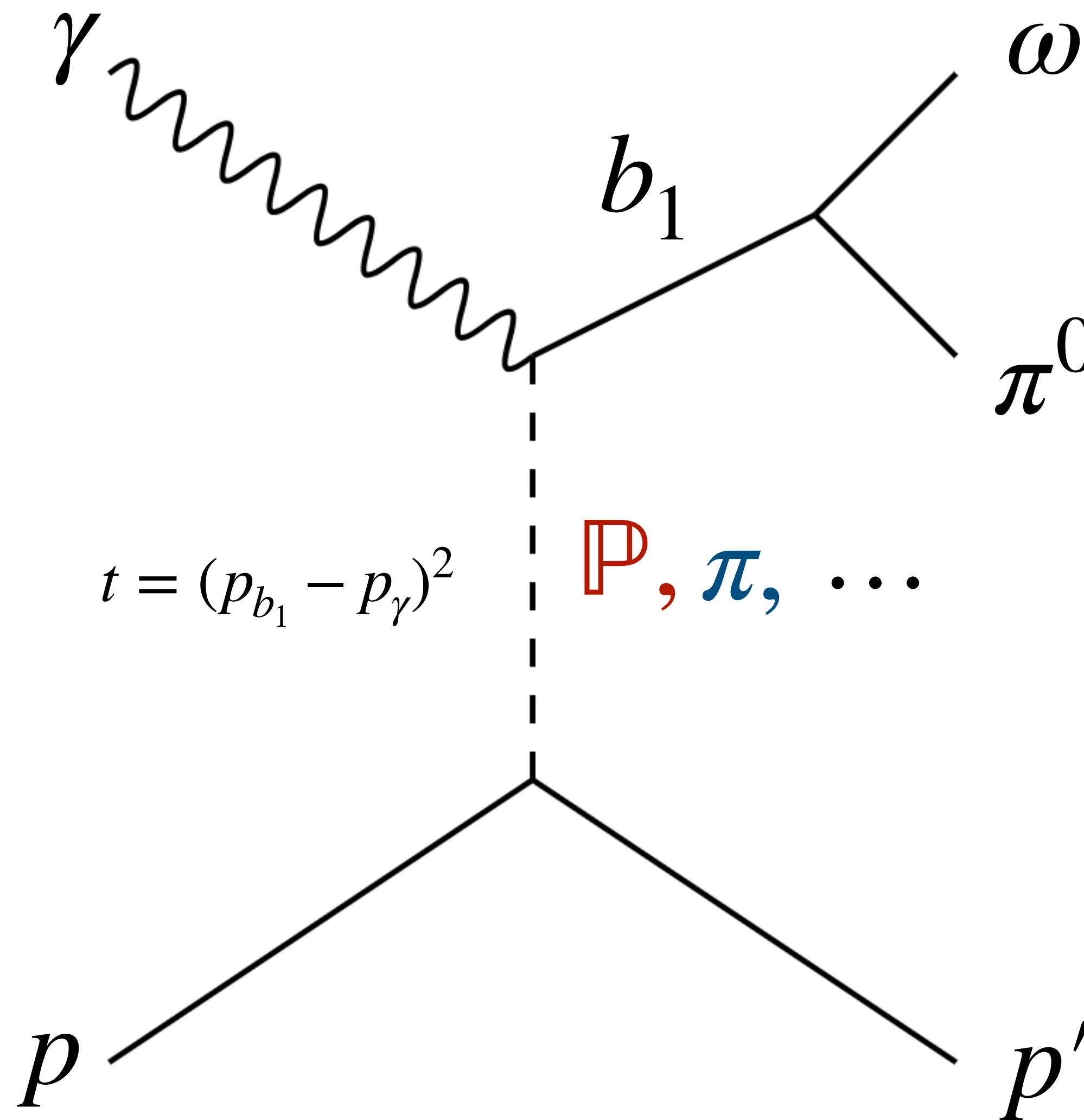
- Large photoproduction cross section - can act as a reference signal for weaker, potentially hybrid signals in the same decay channel
 - For example, multiple hybrids are predicted to have conventional vector (1^{--}) quantum numbers
 - Measurement of their interference with the b_1 could aid in their identification
- The strong $b_1 \rightarrow \omega\pi$ signal also provides a testing ground for this amplitude fit machinery, which can be used for other channels with similar spin structure



Production Mechanisms

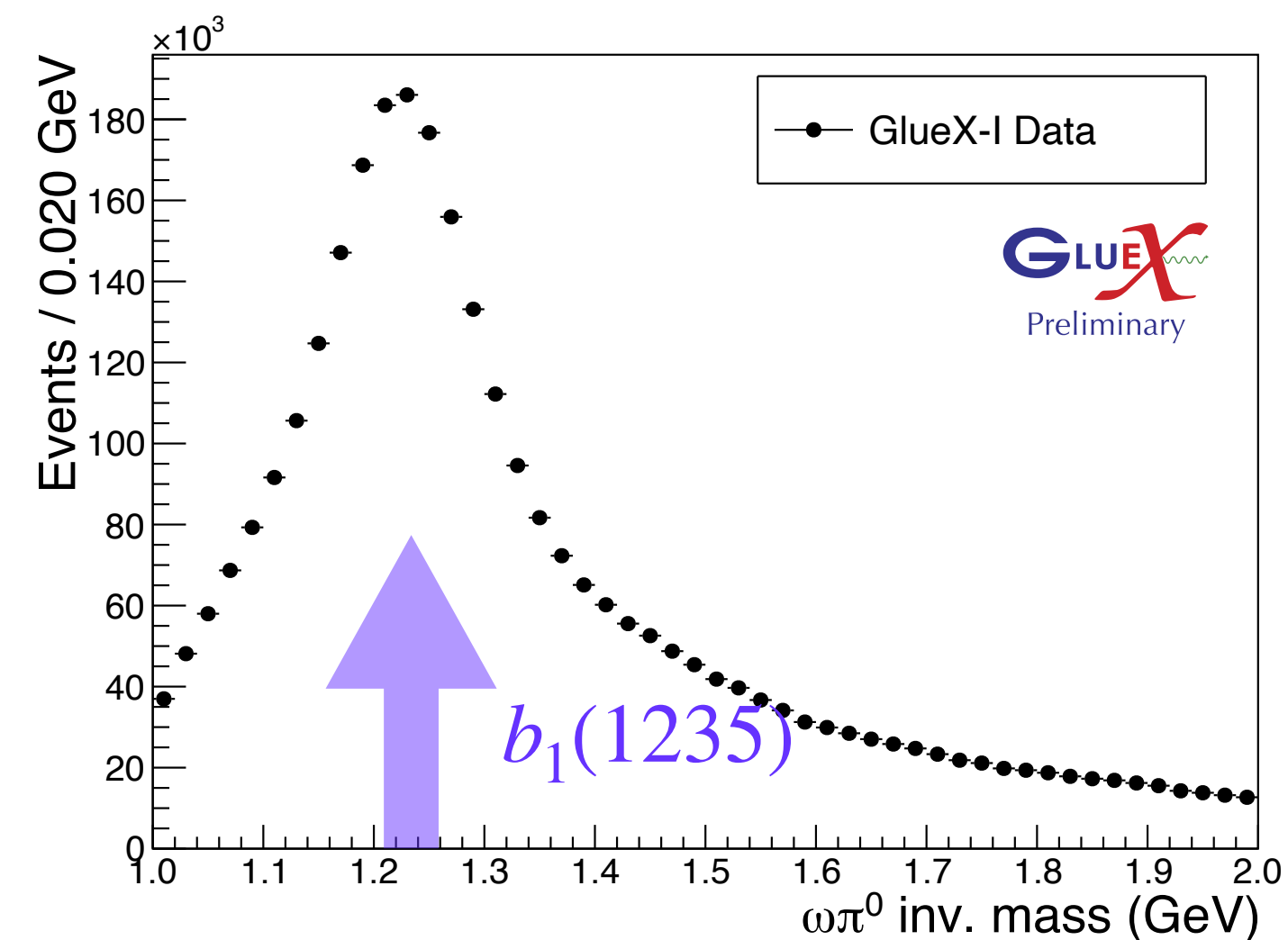
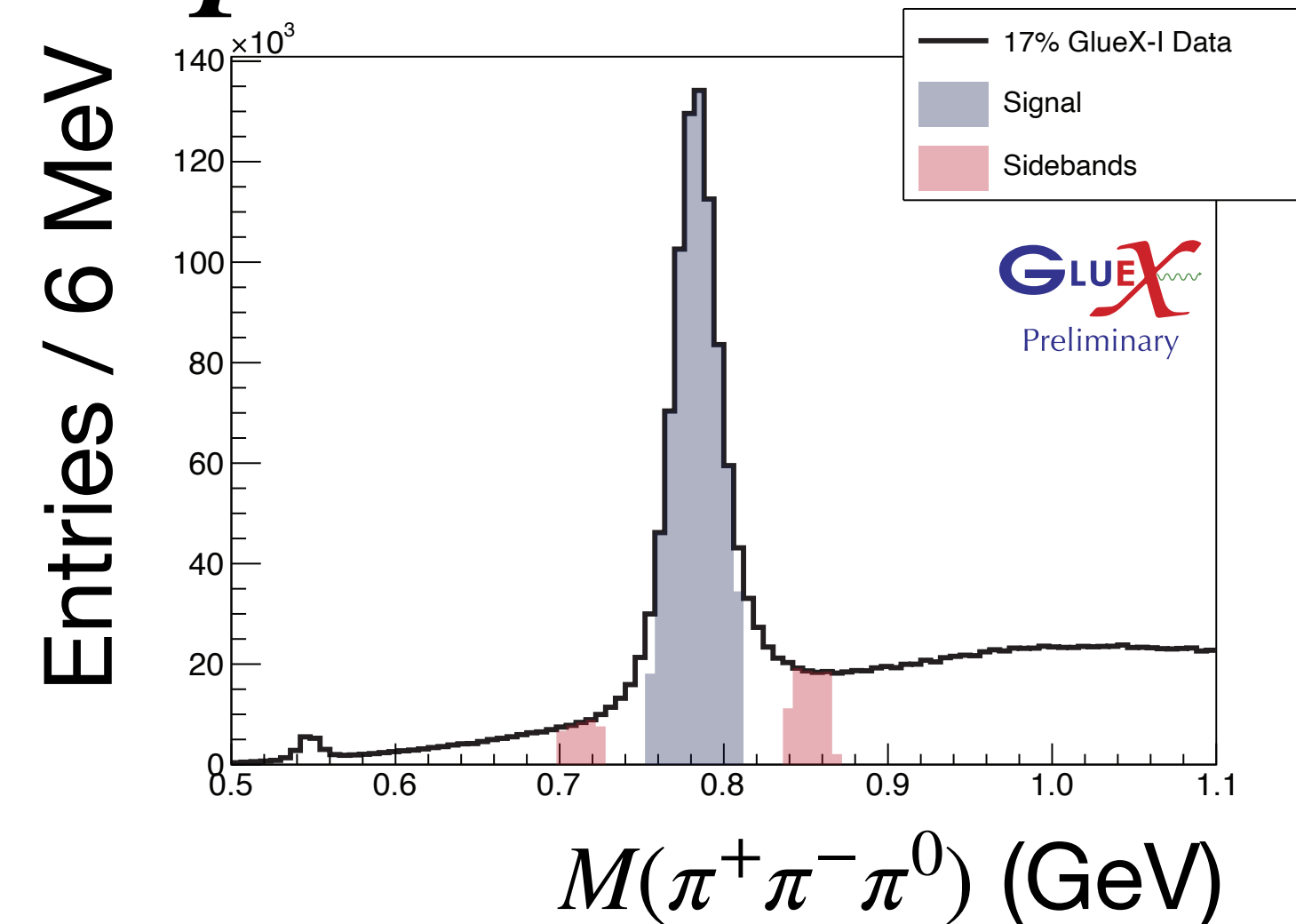
Which ones are preferred in nature?

- Photoproduction at GlueX energies proceeds via exchange of a virtual meson in the t -channel
- By measuring the angle between the production plane and beam polarization, we can extract the naturality of this virtual exchange particle
- Naturality: $P(-1)^J = \pm 1$
 - **Natural** mesons: $\mathbb{P}, \rho, \omega, \phi, f_2, a_2 \dots$
 - **Unnatural** mesons: $\pi, \eta, b_1, h_1 \dots$
- By measuring which type of exchange is preferred in nature, we can place constraints on photocouplings



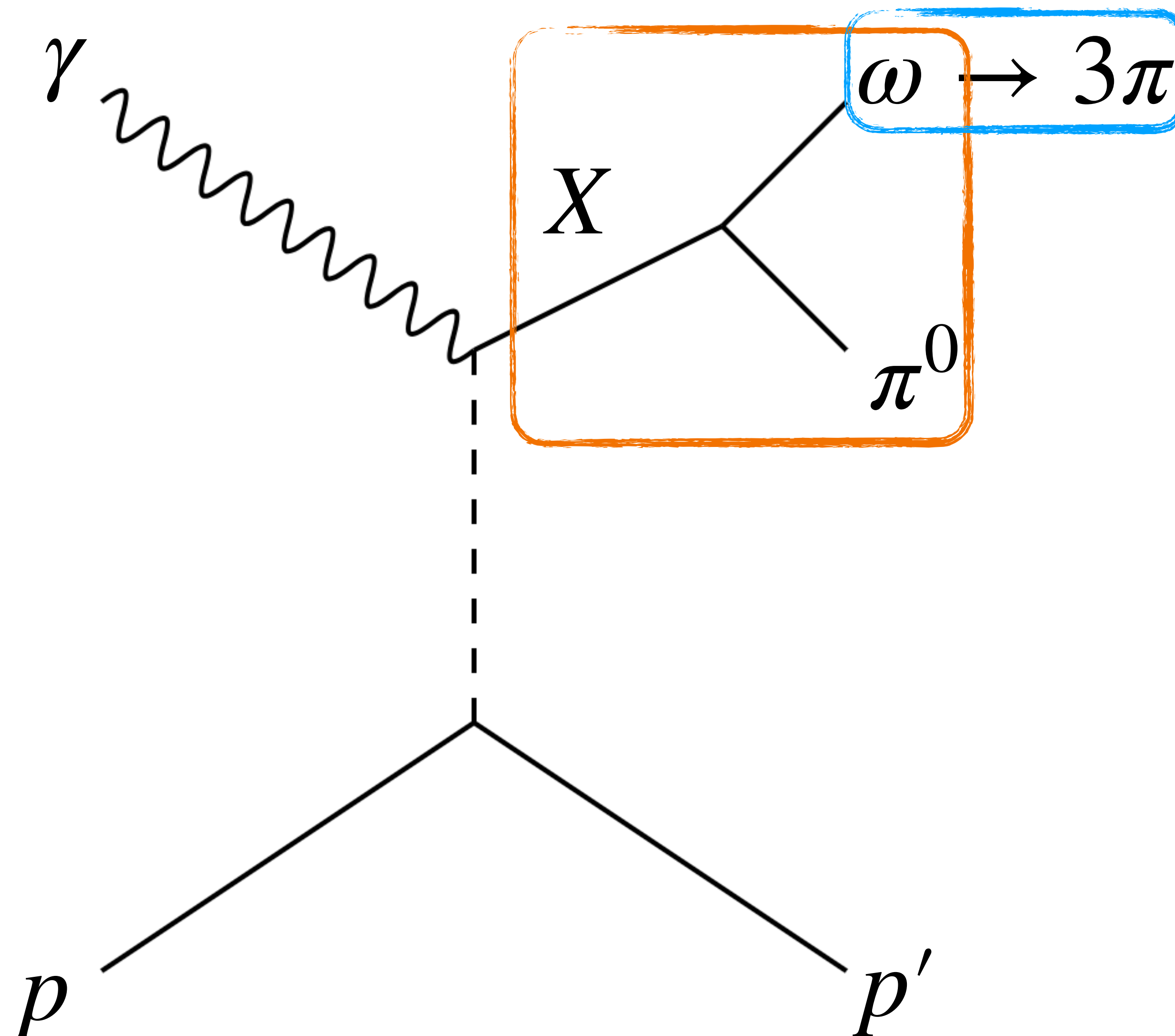
Amplitude Analysis of $\gamma p \rightarrow \omega \pi^0 p$

- Reconstruct exclusive $\pi^+ \pi^- \pi^0 \pi^0 p$ final state
- Sideband subtract the $\pi^+ \pi^- \pi^0$ mass around the ω peak - identifies $\omega \pi^0$ events
- Split data into bins of $M(\omega \pi^0)$ and $-t$
- Perform 5-dimensional angular fit to resonance amplitude model



Production & Decay Angles

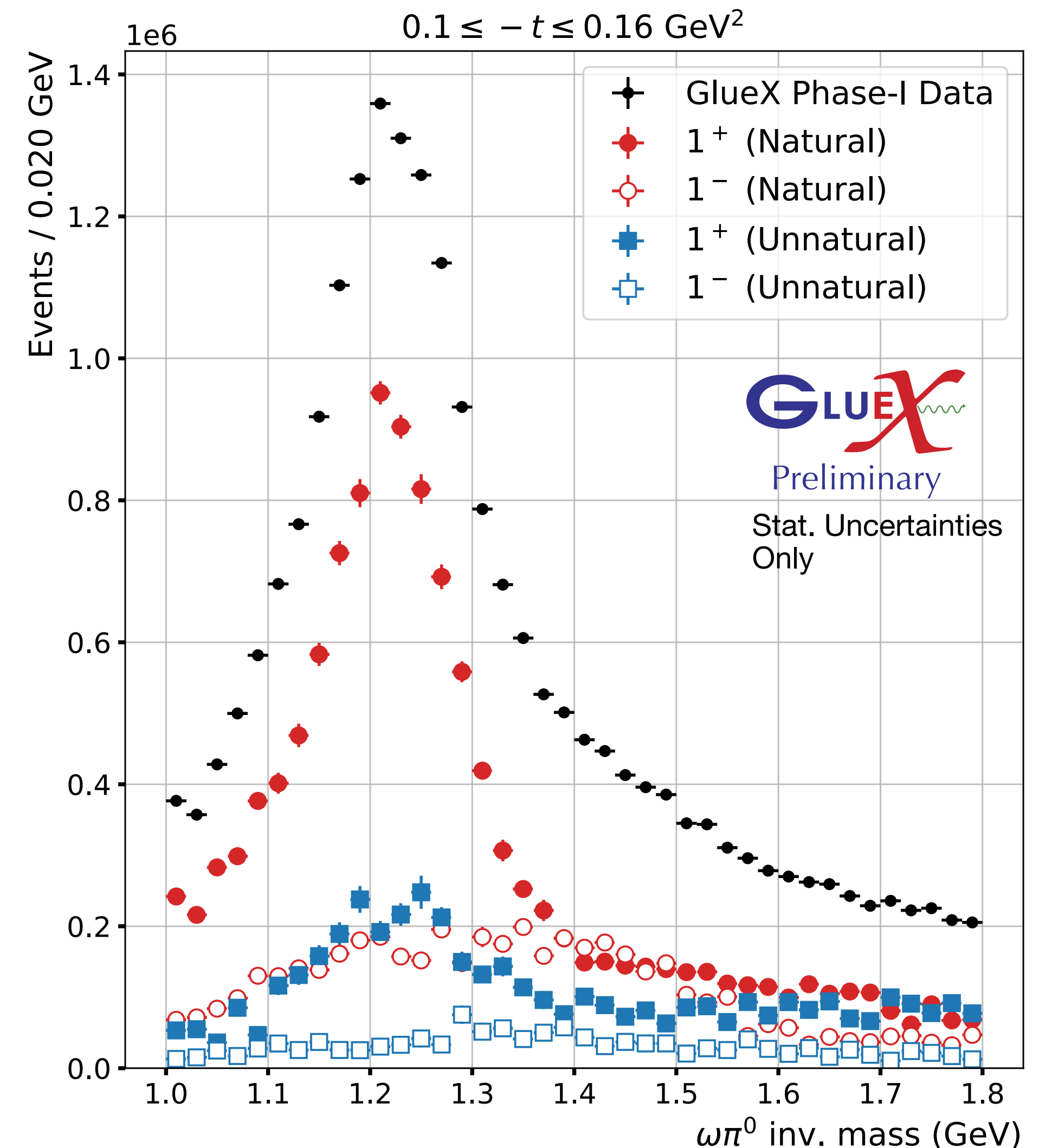
- The production and decay of $\omega\pi^0$ against a proton requires 5 angles to properly describe
- The decay of $X \rightarrow \omega\pi^0$ is described by $\Omega = (\theta, \phi)$
- The decay of $\omega \rightarrow 3\pi$ is described by $\Omega_H = (\theta_H, \phi_H)$
- And Φ is the angle between the beam polarization and production plane



Mass Independent Fit Results

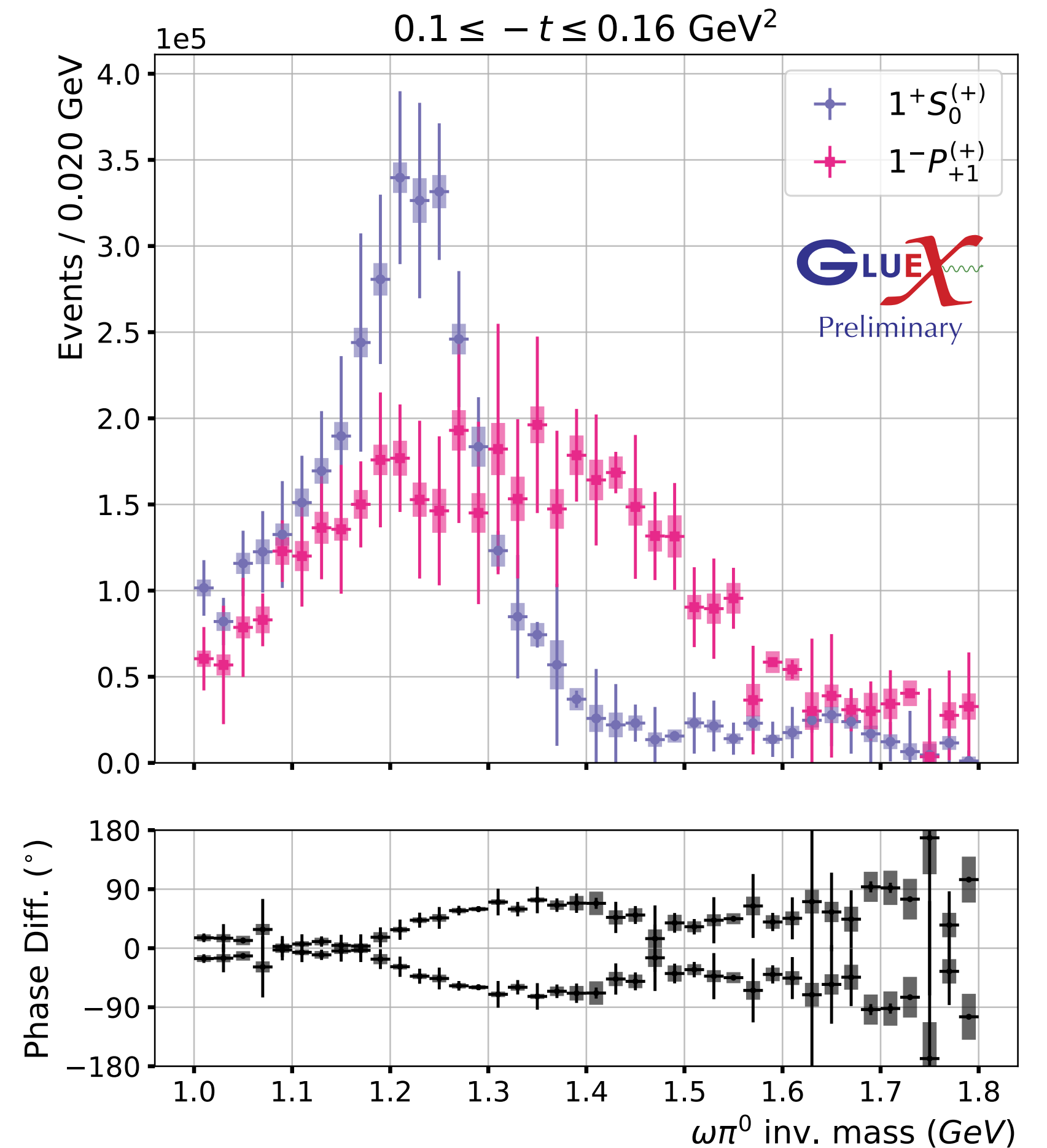
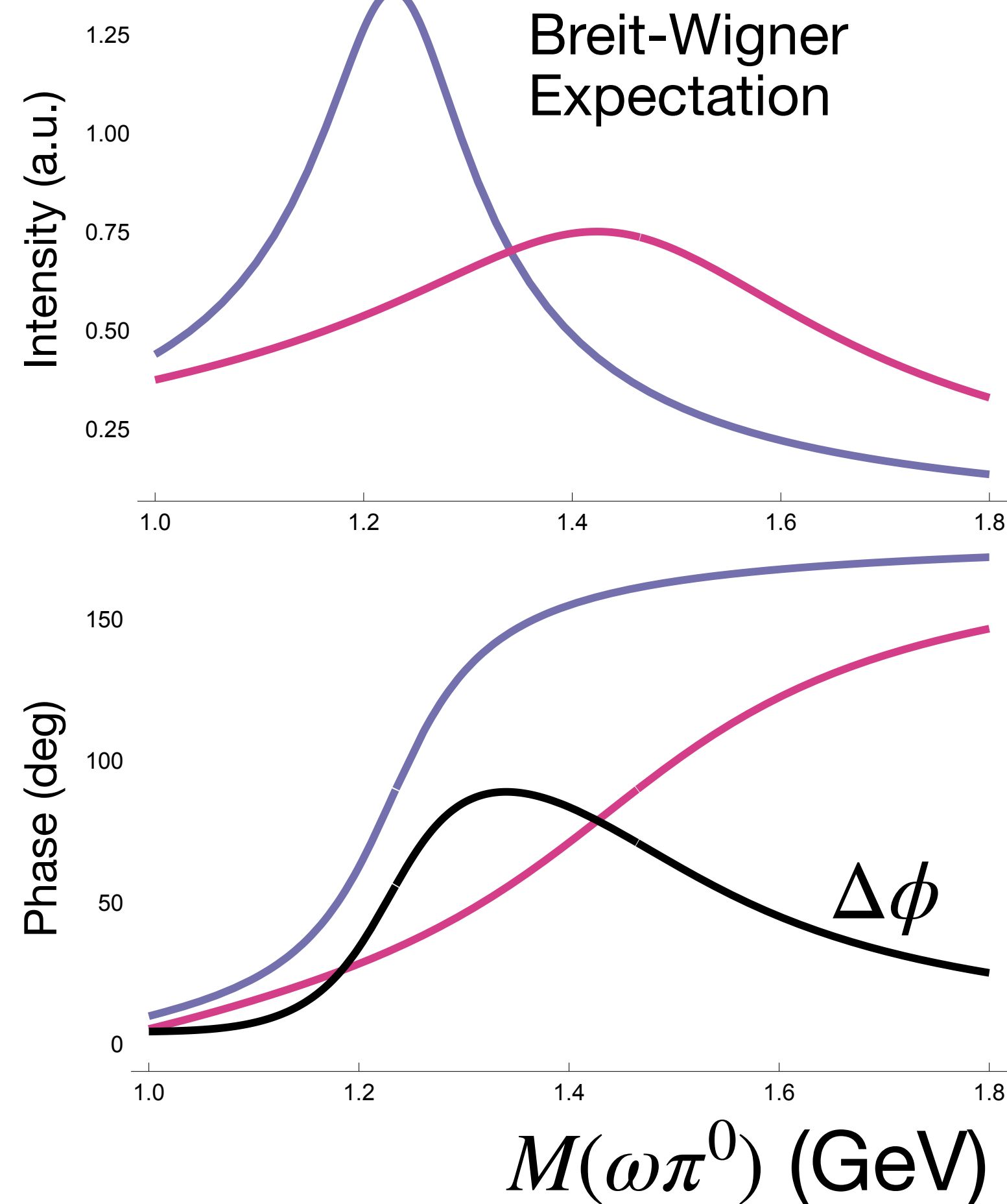
Statistically independent datasets

- Break fit results down by naturality of exchange and quantum numbers of produced wave
- Neutral b_1 ($J^{PC} = 1^{+-}$) production is dominated by **natural** parity exchange
- Vector ($J^{PC} = 1^{--}$) production is also **natural** exchange dominant
- Can study interference between the dominant partial waves of the b_1 and vector



Studying Resonances Through Interference

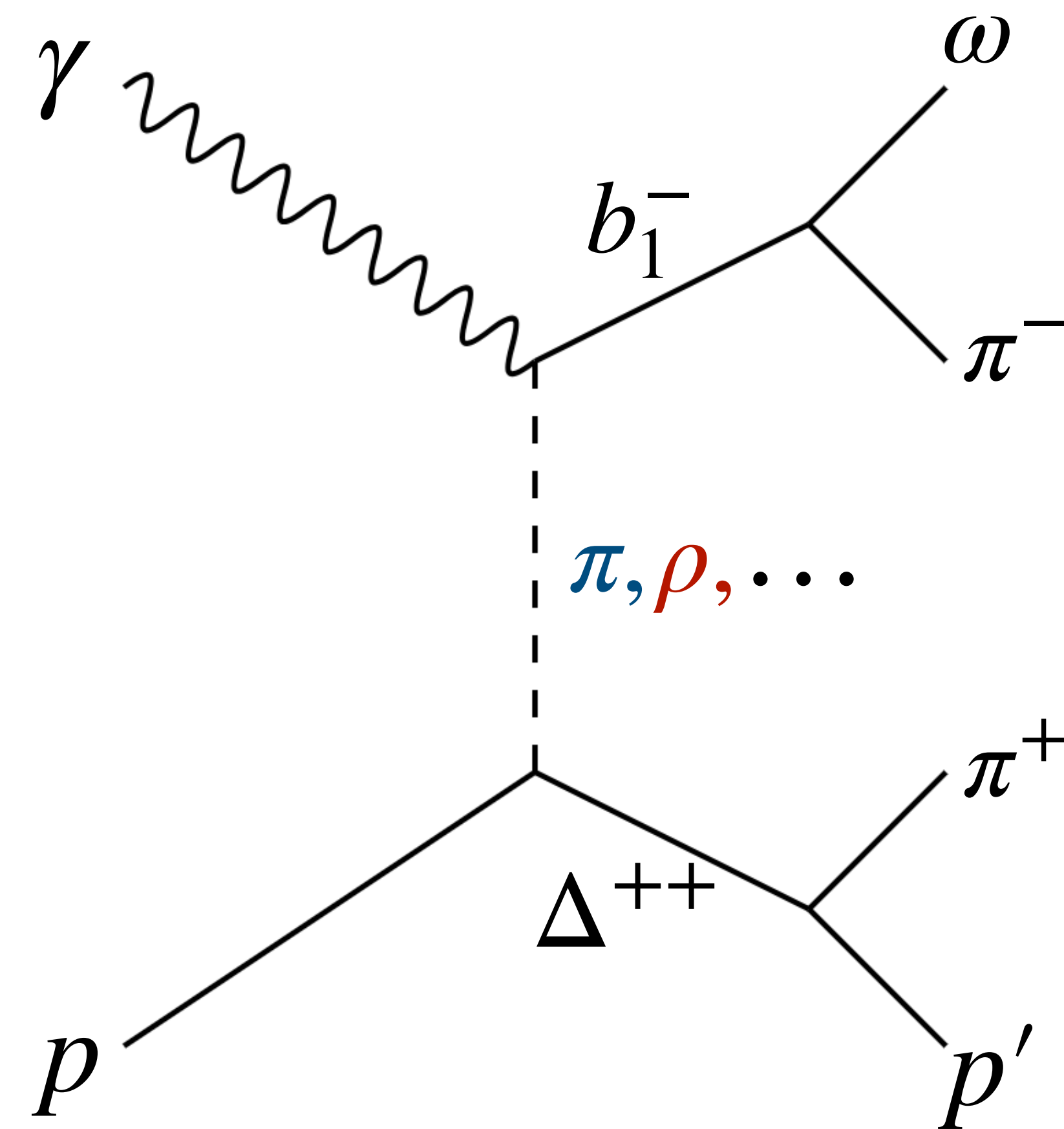
- Dominant partial waves from b_1 and vector contributions
- Phase difference displays resonant behavior
- Analysis assumes nothing about resonances in $\omega\pi^0$



K. Scheuer, Ph.D. Thesis (2026)

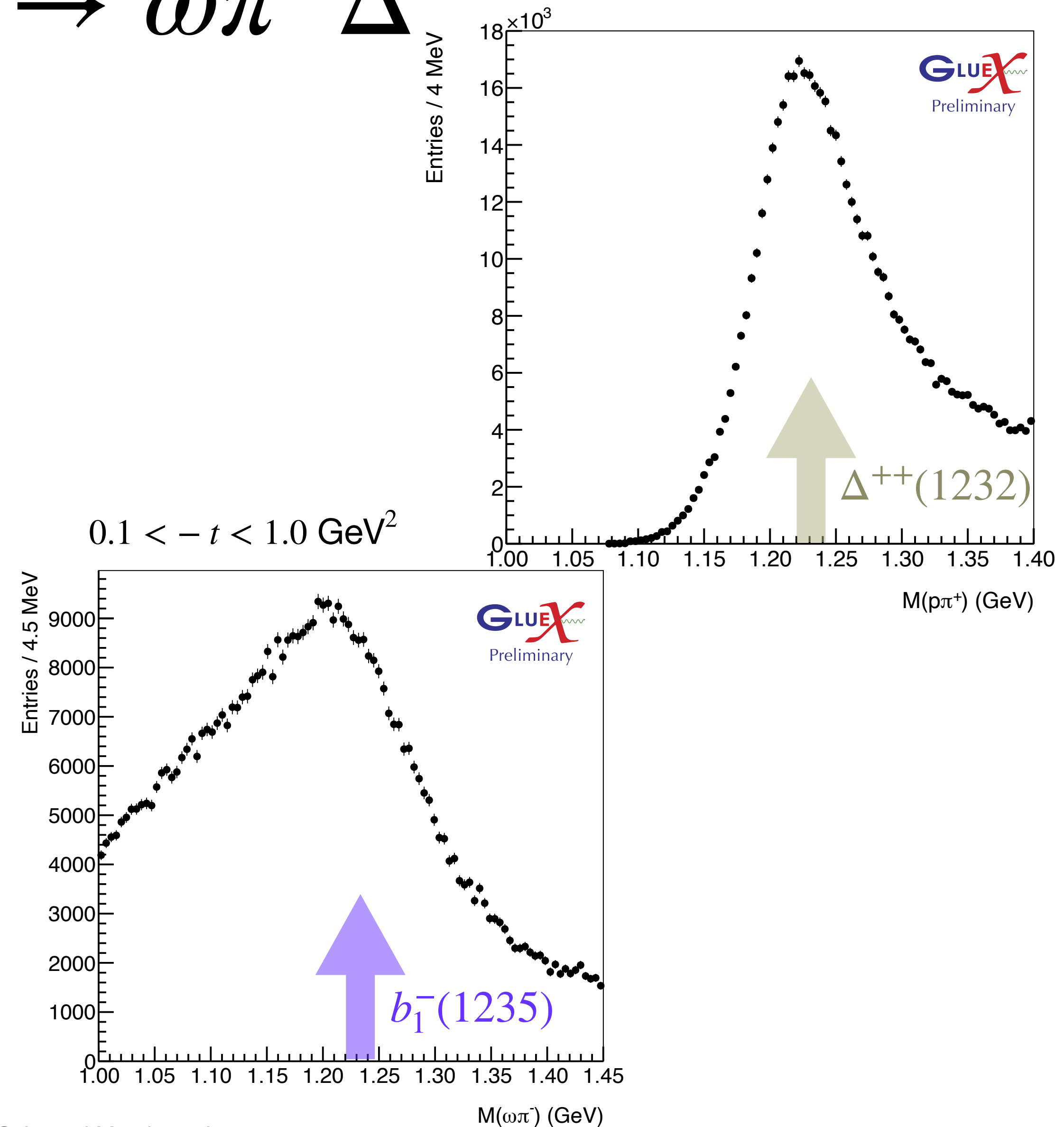
Amplitude Analysis of $\gamma p \rightarrow \omega \pi^- \Delta^{++}$

- The b_1 is an isovector - charged versions can also be studied
- Charged exchange mechanism changes requirements on the virtual exchange particle
 - Nothing electrically neutral, \mathbb{P} exchange not possible
 - C -parity doesn't need to be conserved - ρ exchange is now an option
- Consider b_1^- recoiling off a $\Delta^{++}(1232)$
 - Decay of recoil Δ^{++} introduces another pair of angles



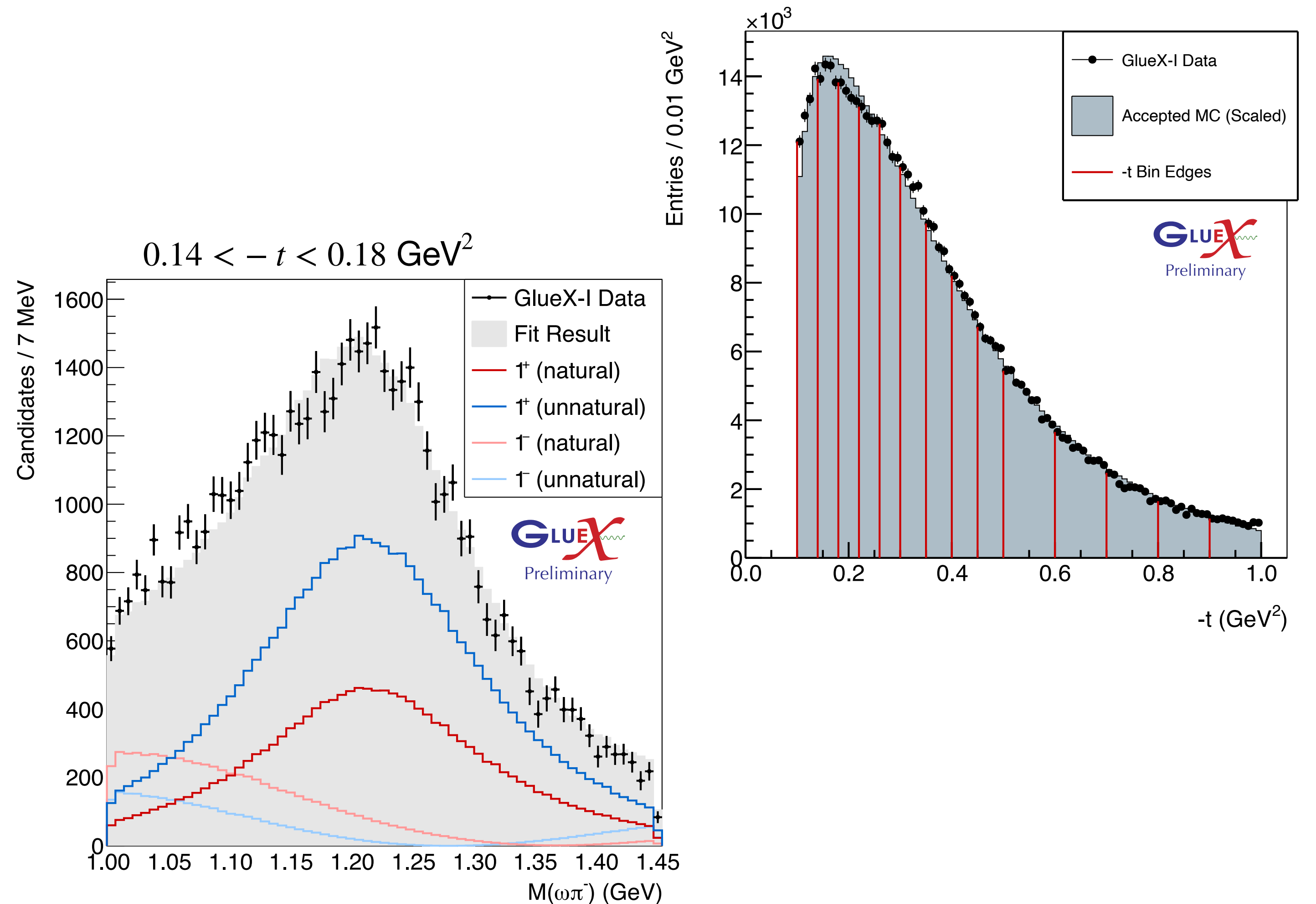
Amplitude Analysis of $\gamma p \rightarrow \omega \pi^- \Delta^{++}$

- Reconstruct exclusive $\omega \pi^- \Delta^{++}$ final state
- Similar sideband subtraction as in the neutral case, with additional requirement that $M(p\pi^+)$ is consistent with production of a $\Delta^{++}(1235)$
- Yields 560k $\omega \pi^-$ events - roughly a factor of 10 fewer than the neutral channel



Amplitude Analysis of $\gamma p \rightarrow \omega \pi^- \Delta^{++}$

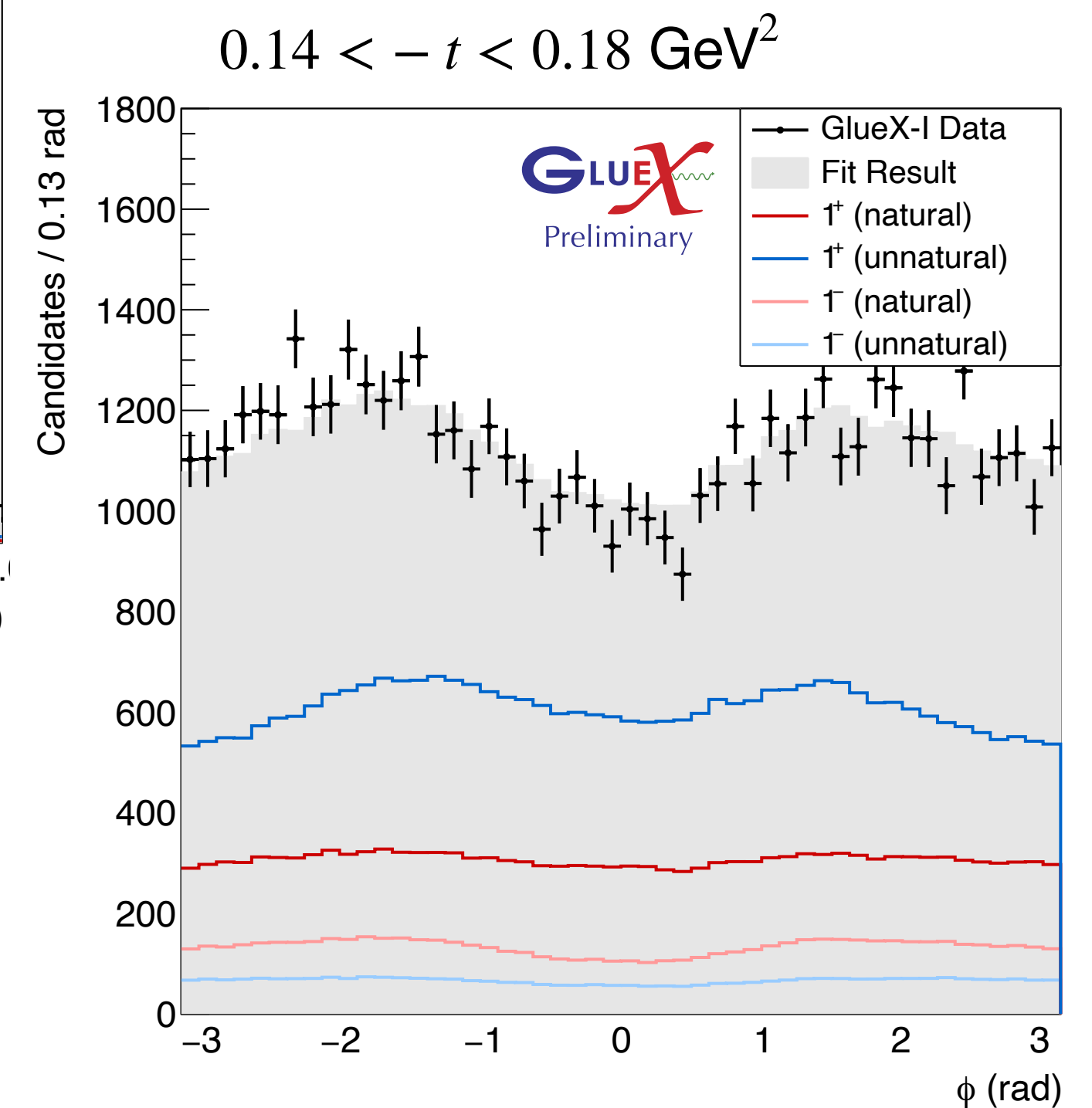
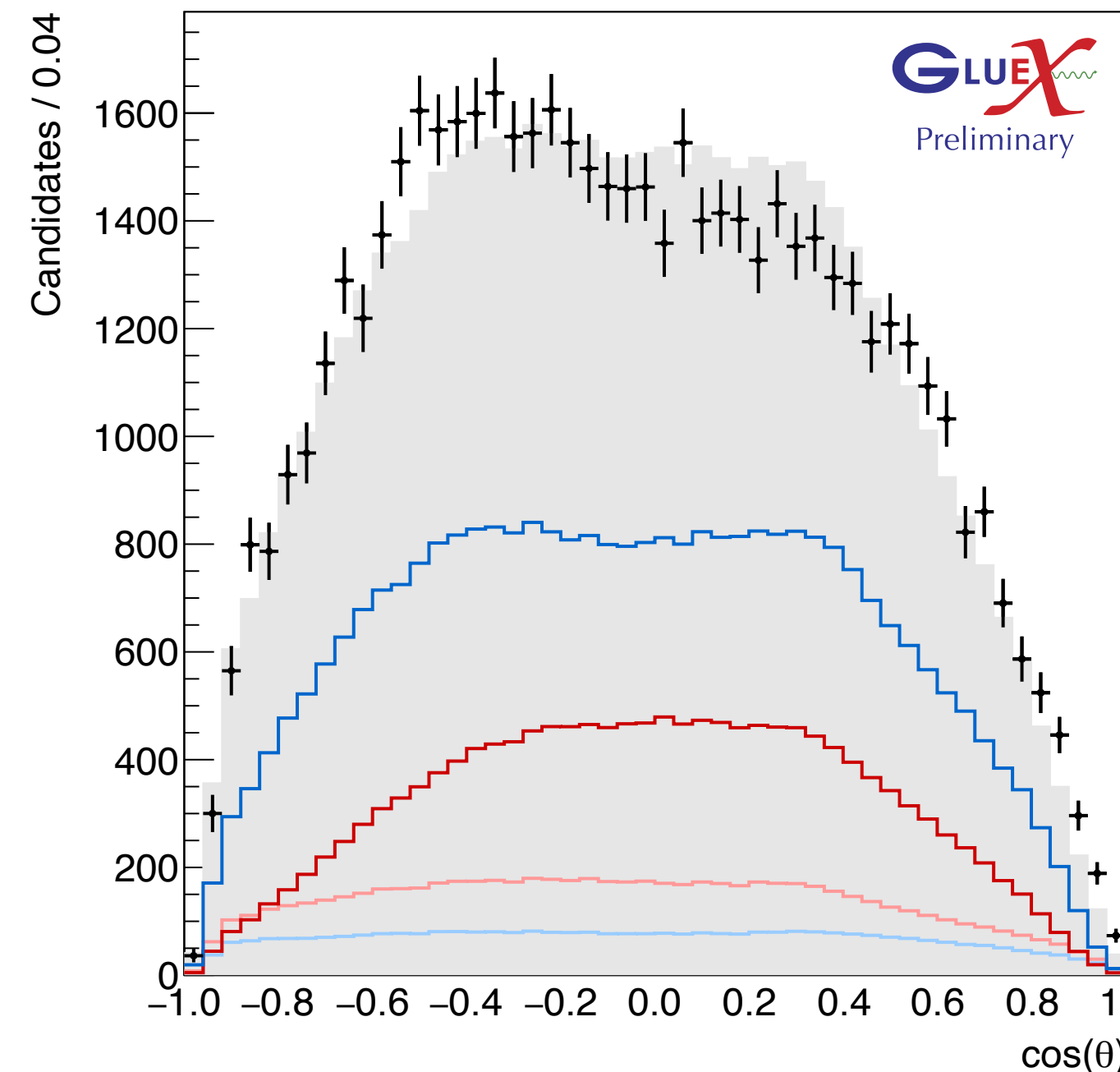
- Divide data into 14 bins in momentum transfer $-t$
- Fit range around the b_1^- mass peak assuming resonant behavior in $\omega\pi^-$
- b_1^- amplitude is described by a relativistic Breit-Wigner function
- Vector ($J^P = 1^-$) amplitude is described by a complex linear function



Amplitude Analysis of $\omega\pi^-$

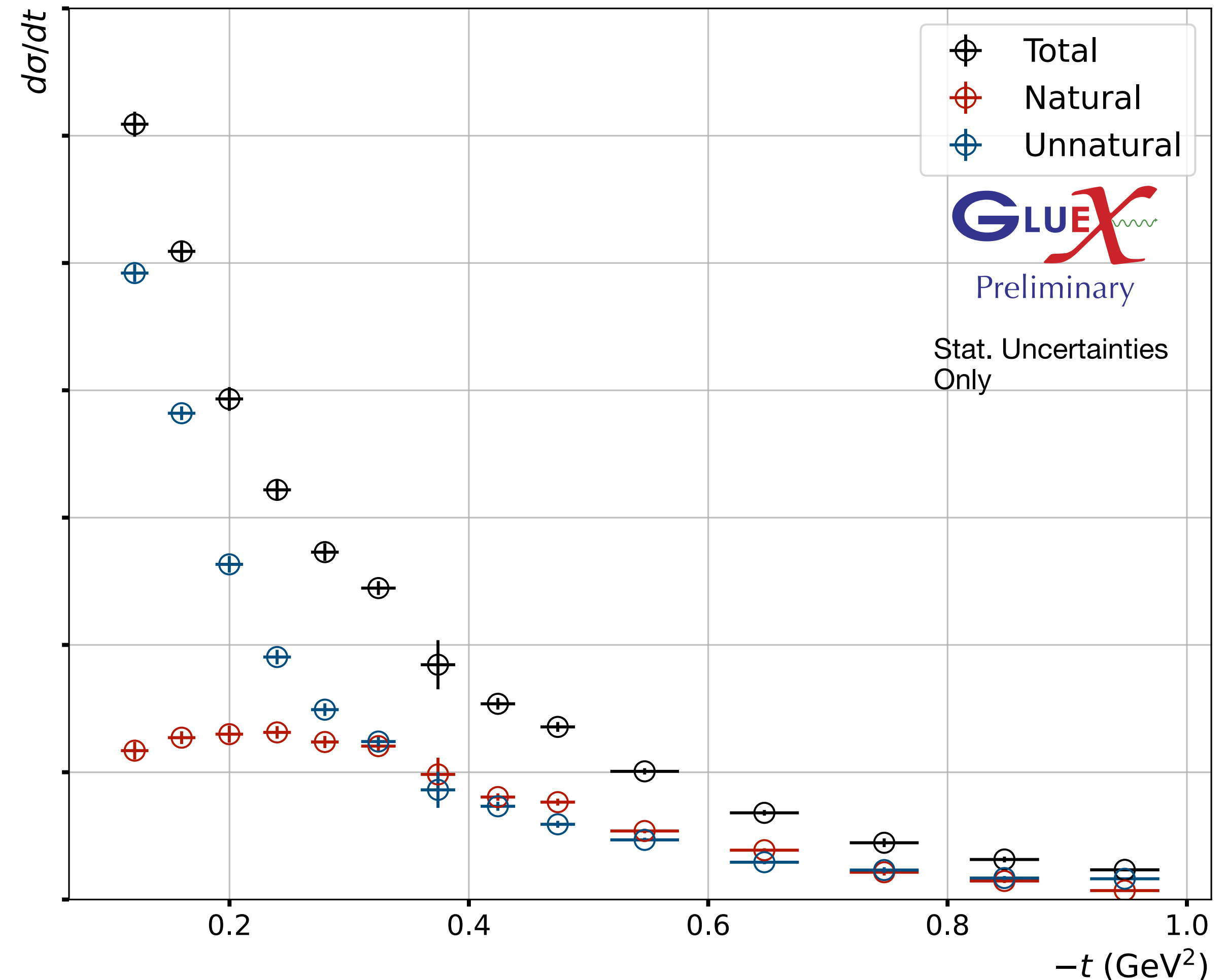
Mass Dependent Fit

- Meson decay angles are described by a resonance amplitude model, similar to the neutral b_1
- Right: Intensities projected onto angles describing the decay $X^- \rightarrow \omega\pi^-$
- $\Delta^{++} \rightarrow p\pi^+$ angular distribution is also included in the fit



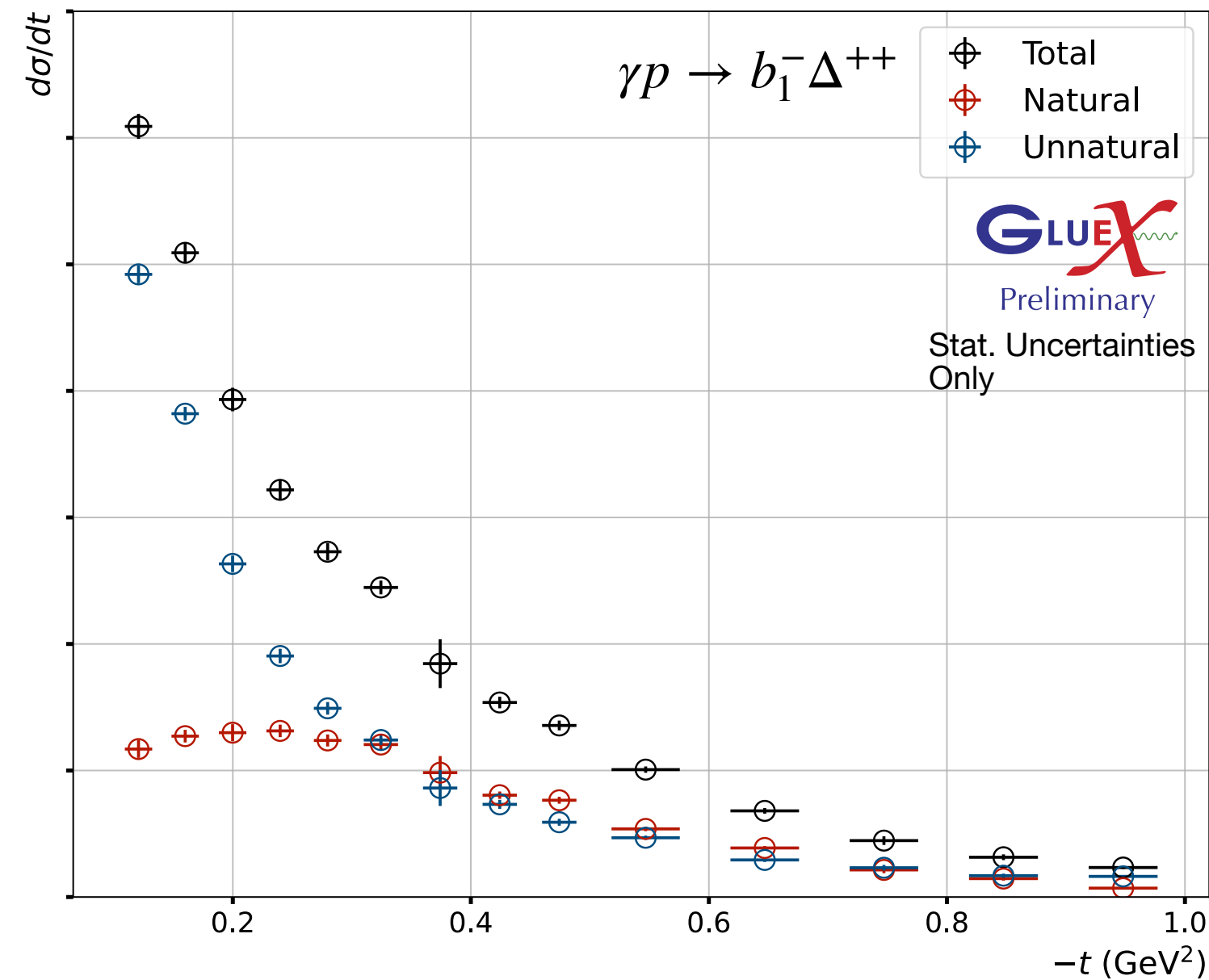
Differential Cross Section of $\gamma p \rightarrow b_1^- \Delta^{++}$

- **Unnatural exchange** is dominant at very low $-t$
 - The most likely exchange particles are π^\pm and ρ^\pm
- Working with JPAC to develop phenomenological models of b_1 production
 - At low $-t$, observe dominance of **unnatural exchange** in the charged mode, while **natural exchange** is dominant in the neutral case

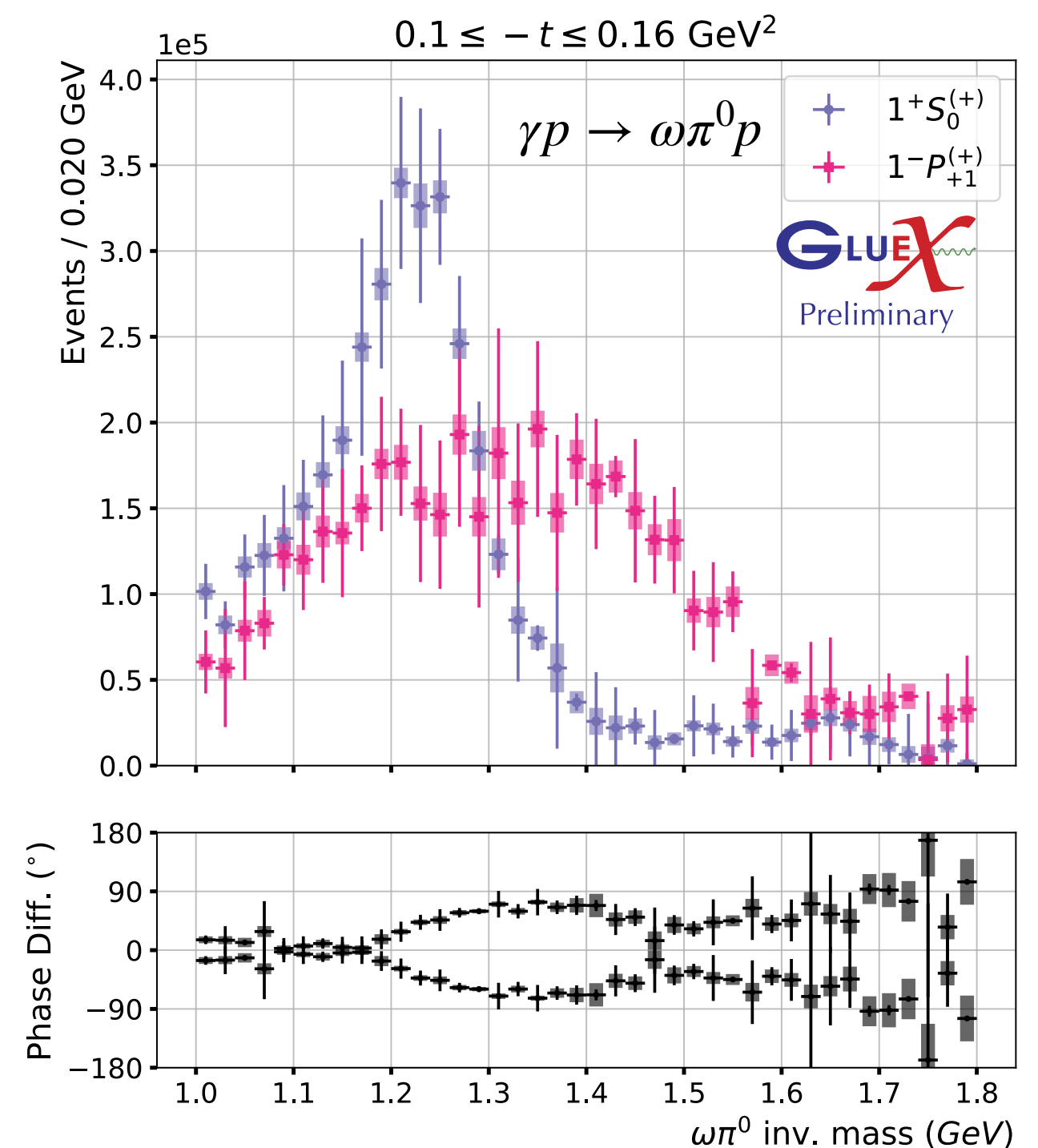


Summary

- Measured the b_1^- cross section, separated by production mechanisms
- **Unnatural exchange** is preferred at low $-t$, unlike in the neutral channel, where **natural exchange** is dominant
- Measured interference between neutral b_1 and excited vector background

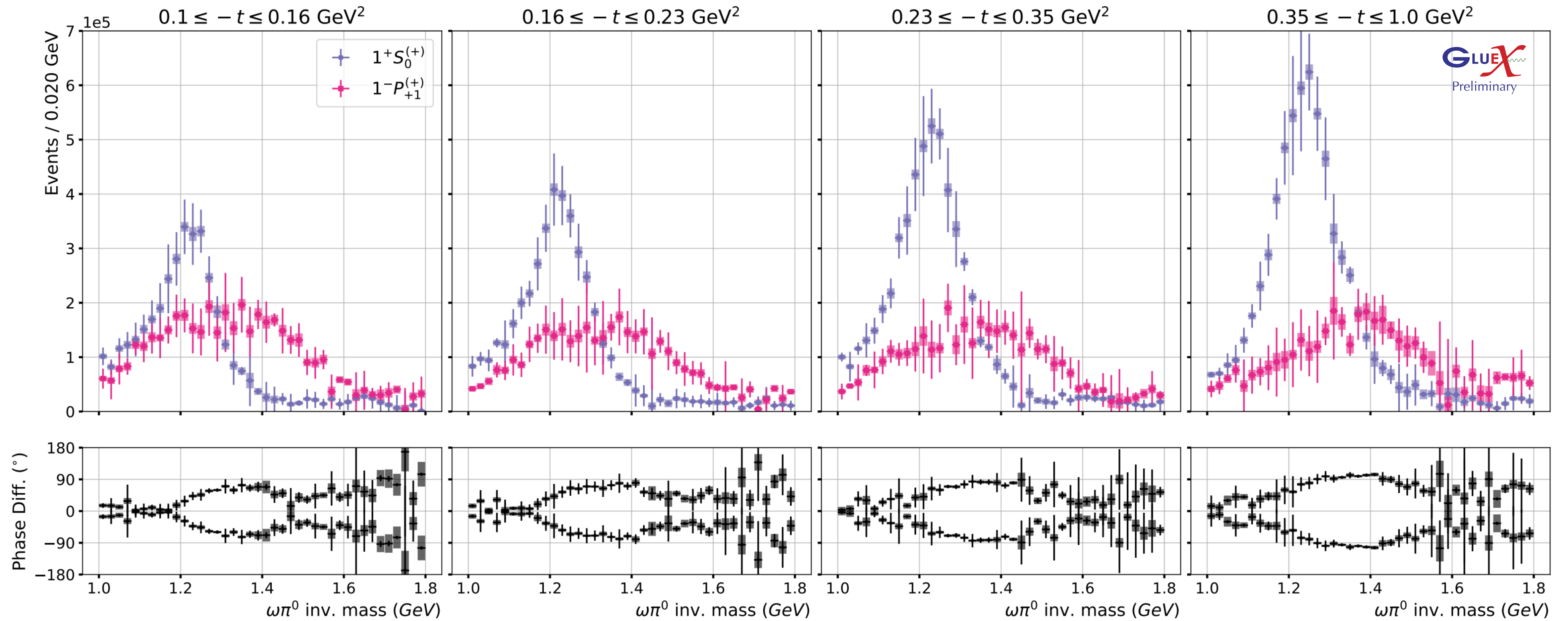


GlueX gratefully acknowledges the support of several funding agencies and computing facilities: gluex.org/thanks



Backup

b_1 Via Analysis of $\omega\pi^0$



K. Scheuer, Ph.D. Thesis (2026)

Cross Section from Amplitude Fits

$$\frac{d\sigma}{dt} = \frac{N_{obs}}{\epsilon \mathcal{L} \mathcal{B}(\omega \rightarrow 3\pi) \mathcal{B}(\Delta^{++} \rightarrow p\pi^+) f_{b_1} f_{\Delta^{++}} \Delta t}$$

↑
Fit result

Vector-Pseudoscalar Amplitudes

Description of the meson vertex

$$\begin{aligned}
 I \propto & (1 - P_\gamma) \left[\left| \sum_{j,m} [J^P]_m^{(-)} \text{Im} Z_m^j (\Phi, \Omega, \Omega_H) \right|^2 + \left| \sum_{j,m} [J^P]_m^{(+)} \text{Re} Z_m^j (\Phi, \Omega, \Omega_H) \right|^2 \right] \\
 & + (1 + P_\gamma) \left[\left| \sum_{j,m} [J^P]_m^{(+)} \text{Im} Z_m^j (\Phi, \Omega, \Omega_H) \right|^2 + \left| \sum_{j,m} [J^P]_m^{(-)} \text{Re} Z_m^j (\Phi, \Omega, \Omega_H) \right|^2 \right]
 \end{aligned}$$

$$Z_m^j (\Phi, \Omega, \Omega_H) = e^{-i\Phi} \sum_{\lambda} F_{\lambda}^j D_{m,\lambda}^{J_j^*} (\Omega) Y_{\lambda}^1 (\Omega_H) G$$

SDME Description

Description of Δ^{++} Decay

$$\begin{aligned}
 W(\Omega_p, \Phi) \propto & \boxed{\rho_{33}^0} \sin^2 \theta_p + \boxed{\rho_{11}^0} \left(\frac{1}{3} + \cos^2 \theta_p \right) - \frac{2}{\sqrt{3}} \boxed{\text{Re}\rho_{31}^0} \sin 2\theta_p \cos \phi_p - \frac{2}{\sqrt{3}} \boxed{\text{Re}\rho_{3-1}^0} \sin^2 \theta_p \cos 2\phi_p \\
 & - P_\gamma \cos 2\Phi \left[\boxed{\rho_{33}^1} \sin^2 \theta_p + \boxed{\rho_{11}^1} \left(\frac{1}{3} + \cos^2 \theta_p \right) - \frac{2}{\sqrt{3}} \boxed{\text{Re}\rho_{31}^1} \sin 2\theta_p \cos \phi_p - \frac{2}{\sqrt{3}} \boxed{\text{Re}\rho_{3-1}^1} \sin^2 \theta_p \cos 2\phi_p \right] \\
 & - P_\gamma \sin 2\Phi \left[\frac{2}{\sqrt{3}} \boxed{\text{Im}\rho_{31}^2} \sin 2\theta_p \sin \phi_p + \frac{2}{\sqrt{3}} \boxed{\text{Im}\rho_{3-1}^2} \sin^2 \theta_p \sin 2\phi_p \right]
 \end{aligned}$$

NB: $\rho_{11}^0 + \rho_{33}^0 = \frac{1}{2}$ and $\Sigma = 2(\rho_{11}^1 + \rho_{33}^1)$